JCB Article

Modulation of the F-actin cytoskeleton by c-Abl tyrosine kinase in cell spreading and neurite extension

Pamela J. Woodring,[1] E. David Litwack,[1] Dennis D.M. O'Leary,[1] Ginger R. Lucero,[1] Jean Y.J. Wang,[2] and Tony Hunter[1]

[1]The Salk Institute, La Jolla, CA 92037
[2]Division of Biology and the Cancer Center, University of California at San Diego, La Jolla, CA 92093

The nonreceptor tyrosine kinase encoded by the c-Abl gene has the unique feature of an F-actin binding domain (FABD). Purified c-Abl tyrosine kinase is inhibited by F-actin, and this inhibition can be relieved through mutation of its FABD. The c-Abl kinase is activated by physiological signals that also regulate the actin cytoskeleton. We show here that c-Abl stimulated the formation of actin microspikes in fibroblasts spreading on fibronectin. This function of c-Abl is dependent on kinase activity and is not shared by c-Src tyrosine kinase. The Abl-dependent F-actin microspikes occurred under conditions where the Rho-family GTPases were inhibited. The FABD-mutated c-Abl, which is active in detached fibroblasts, stimulated F-actin microspikes independent of cell attachment. Moreover, FABD-mutated c-Abl stimulated the formation of F-actin branches in neurites of rat embryonic cortical neurons. The reciprocal regulation between F-actin and the c-Abl tyrosine kinase may provide a self-limiting mechanism in the control of actin cytoskeleton dynamics.

Introduction

The actin cytoskeleton is a dynamic network that is regulated by a variety of extracellular signals. Growth factors or extracellular matrix (ECM)* proteins transmit signals through actin to modulate intracellular trafficking, cell morphology, cell migration, and process extension (Zigmond, 1996). Actin cytoskeletal rearrangements, in turn, influence the function of signal transduction pathways stimulated by growth factors (Sotiropoulos et al., 1999). Dynamic structural alterations of the actin cytoskeleton require polymerization, depolymerization, stabilization, branching, and severing of actin filaments. Rapid extension and retraction of filopodia and lamellipodia through F-actin assembly and disassembly is the driving force that permits cells to explore and navigate in response to extracellular cues. This is evident in cell spreading and migration, as well as in neurons extending dendrites and axons. Protrusive activity at the leading edge of a migrating cell or at the growth cone of an axon requires regulated actin polymerization. Sites of branch formation on axon shafts behave as motile structures as well, characterized by rapid actin cytoskeletal reorganization (Kalil et al., 2000). Recent research had identified a number of key components essential for control of actin polymerization and depolymerization including profilin, Arp2/3, WASp/Scar/WAVE, actin capping proteins, actin severing proteins, and Rho family GTPases (Pollard et al., 2000; Bear et al., 2001). However, the molecular mechanisms that are responsible for regulating these components and ultimately actin dynamics during motile cellular processes remain to be characterized.

The c-Abl gene encodes a nonreceptor tyrosine kinase that contains a binding site for F-actin (McWhirter and Wang, 1993; Van Etten et al., 1994; Woodring et al., 2001). Cells deficient for c-Abl show a reduced and delayed ruffling response to PDGF (Plattner et al., 1999). Inhibition of c-Abl kinase activity with signal transduction inhibitor 571 (STI571) can increase cell migration measured in Boyden chamber assays (Frasca et al., 2001; Kain and Klemke, 2001). The *abl* gene is conserved in invertebrates, and the *Drosophila* Abl (dAbl) functions in axon guidance (Lanier and Gertler, 2000). The c-Abl tyrosine kinase can phosphorylate proteins such as Mena, paxillin, SH3-SH2 containing adaptor proteins (e.g., Crk, p130Cas, disabled), and Cdk5 that are involved in the regulation of focal adhesions and F-actin structure and dynamics (Van Etten, 1999). c-Abl

The online version of this article contains supplemental material.

Address correspondence to Pamela J. Woodring, The Salk Institute, 10010 North Torrey Pines Rd., La Jolla, CA 92037-1099. Tel.: (858) 453-4100. Fax: (858) 457-4765. E-mail: woodring@salk.edu

*Abbreviations used in this paper: CTD, COOH-terminal repeat domain; DKO, double knock out; ECM, extracellular matrix; FABD, F-actin binding domain; GST, glutathione *S*-transferase; STI571, signal transduction inhibitor 571.

Key words: Abl−/− Arg−/− fibroblasts; latrunculin; STI571; fibronectin cell spreading; F-actin microspikes

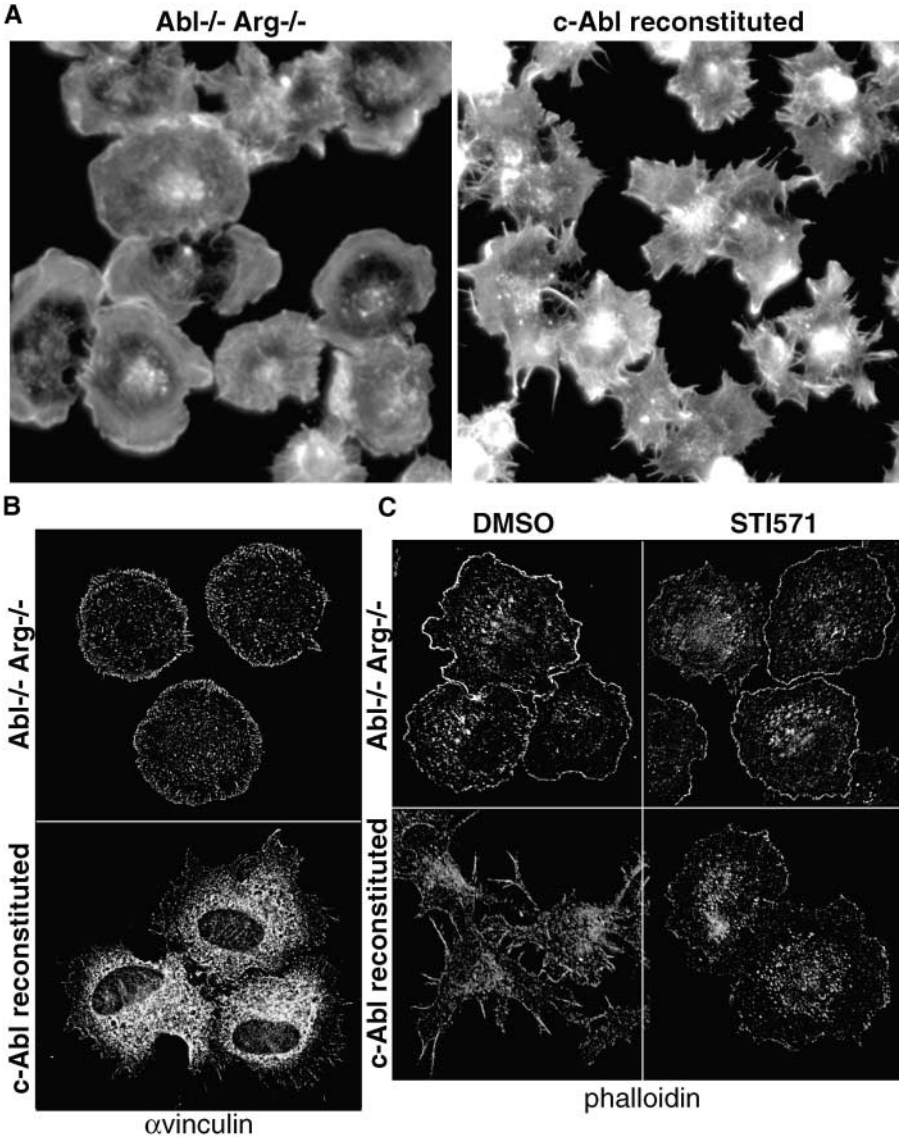

Figure 1. **c-Abl activity contributes to cell spreading.** (A) Double knock out cells (Abl−/− Arg−/−) reconstituted with vector (left) or c-Abl (right) were detached, held in suspension 45 min, then plated onto a fibronectin-coated surface for 20 min. Cells were fixed and stained with TRITC-conjugated phalloidin to visualize the F-actin cytoskeleton. (B) Cells were treated as in A except they were fixed at 35 min after plating onto fibronectin and αvinculin/α-mouse Texas red (Sigma-Aldrich) was used for staining to visualize focal contacts. (C) Double knock out cells reconstituted with vector (top) or c-Abl (bottom) were pretreated with either the vehicle control, DMSO (left) or 3 μM STI571 (right). In the continued presence of DMSO or STI571 cells were detached, held in suspension for 45 min, and replated onto a fibronectin-coated surface for 30 min. Fixed cells were stained with FITC-conjugated phalloidin. (D) Src knock out cells (Src−/−) reconstituted with vector (top left) or c-Src (top right) were detached and spread onto a fibronectin-coated surface, then stained as in A. The indicated cells were pretreated with 3 μM STI571 or 1 μM SU6656 (middle). Bottom panels show 293T cells overexpressing activated Src(Y529F). 24 h after transfection cells were pretreated with DMSO (left) or STI571 (right). Cells were detached and replated onto fibronectin as in A. Transfected cells were located by staining with αSrc/FITC-αmouse, and the actin cytoskeleton was visualized with TRITC-phalloidin.

can also associate with WAVE1 (Westphal et al., 2000), an activator of the Arp2/3 complex. Furthermore, some extracellular signals that activate c-Abl also cause alterations in the F-actin cytoskeleton. For example, clustering of integrins by ECM proteins activates c-Abl (Lewis et al., 1996; Lewis and Schwartz, 1998; Woodring et al., 2001) and promotes cell attachment and spreading. Conversely, c-Abl mutated in the F-actin binding domain (FABD) is active independent of integrins. Indeed, F-actin itself is an inhibitor of the c-Abl activity in vitro (Woodring et al., 2001). Altogether, these studies point toward a reciprocal regulation between c-Abl and F-actin in which c-Abl regulates and is regulated by the F-actin cytoskeleton.

We report here that F-actin surface protrusions are stimulated by c-Abl tyrosine kinase in spreading fibroblasts and along growing axons. In both systems, increased c-Abl activity correlates with increased quantities of F-actin microspike protrusions. The positive effect of c-Abl on the formation of F-actin microspikes may be balanced by the negative effect of F-actin on c-Abl kinase activity to limit the extent and duration of these F-actin protrusions. Thus, our results suggest a self-limiting mechanism where F-actin and c-Abl exert rapid effects on each other to regulate the dynamics of cell morphology and motility.

Results

c-Abl modulates cell spreading on fibronectin

Integrin–ECM engagement can activate mechanisms to mediate cell adhesion and direct cell migration (Hynes, 1992). The regulation of actin cytoskeleton by ECM proteins is readily observed when fibroblasts spread on the ECM. To investigate if c-Abl activity contributes to cell spreading on ECM (fibronectin), we used fibroblasts established from Abl−/− Arg−/− (double knock out [DKO]) E9.5 mouse embryos (Koleske et al., 1998). DKO cells were stably reconstituted with endogenous levels of wild-type c-Abl using retroviral infection followed by selection for 4 wk. The resulting polyclonal population of cells contained a relatively even distribution c-Abl expression comparable to the level of c-Abl found in NIH3T3 cells (unpublished data). The overall morphology of DKO cells reconstituted with c-Abl or reconstituted with pMSCV empty vector appeared quite similar at steady-state. However, we observed striking differences in their morphology at early times (between 0–40 min) of spread-

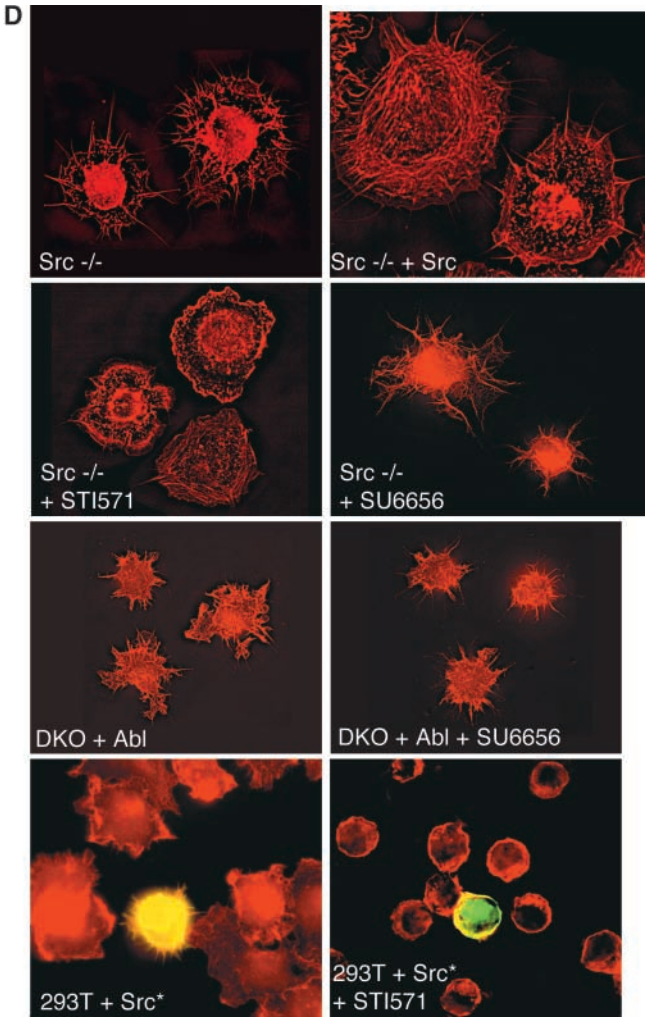

Figure 1 (continued)

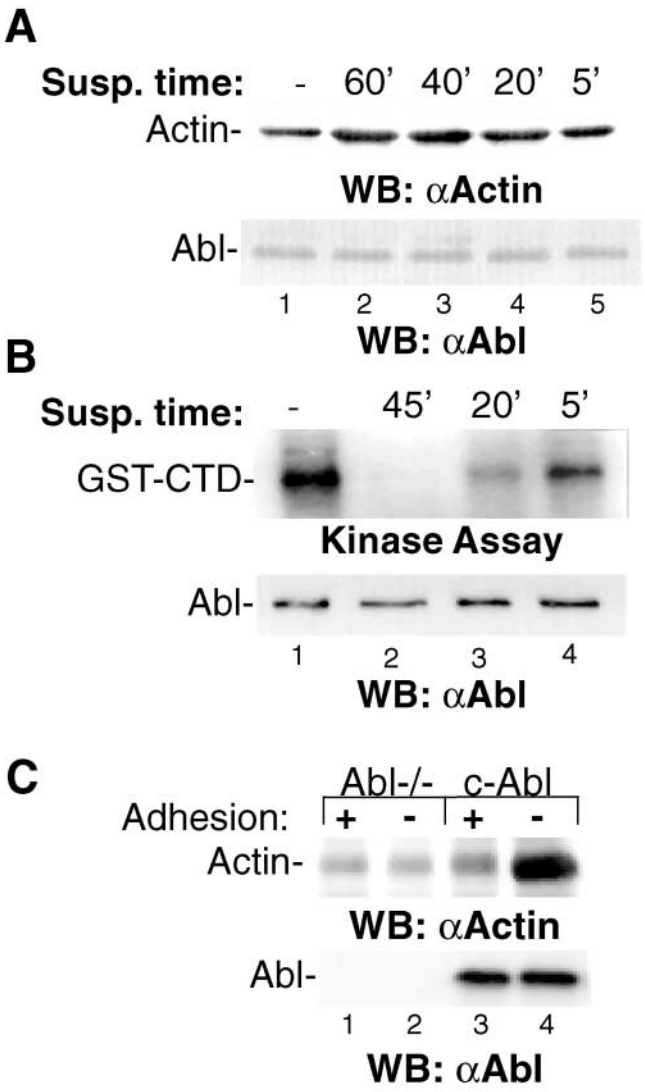

Figure 2. **Association of c-Abl with the F-actin cytoskeleton in detached cells.** (A) c-Abl was immunoprecipitated (αFLAG-M2; Sigma-Aldrich) from c-Abl–reconstituted Abl−/− fibroblasts that were held in suspension for the indicated time (lanes 2–5) or reattached onto a fibronectin coated surface (lane 1). Immunoprecipitates were examined for quantity of associated actin by immunoblotting (αactin, Sigma-Aldrich; α8E9, BD PharMingen). (B) Performed as in A, immunoprecipitations were analyzed for c-Abl kinase activity using glutathione *S*-transferase (GST)–COOH-terminal domain (CTD) of RNA polymerase II as a specific Abl substrate (Baskaran et al., 1993, 1996; Gong et al., 1999; Woodring et al., 2001). (C) As a control, we performed immunoprecipitations from vector reconstituted Abl−/− fibroblasts (lanes 1 and 2) versus c-Abl reconstituted (lanes 3 and 4). Fibroblasts were held in suspension for 45 min and immunoprecipitation was as in A.

ing on fibronectin in the absence of serum. Fig. 1 A shows F-actin (phalloidin) staining of each cell type spread on a fibronectin surface for 20 min. Although the DKO+vector cells did spread, the morphology of their cytoskeleton was quite distinct from that of the DKO+c-Abl cells. The DKO+vector cells had a more rounded morphology compared with the DKO+c-Abl cells, which had F-actin rich membrane extensions (microspikes) around their perimeter resulting in a spiked, stellate morphology. Similar microspikes were also observed in early passage mouse embryo Abl−/− 3T3 fibroblasts reconstituted with c-Abl (unpublished data). We quantified microspikes during spreading among four independently derived polyclonal populations of reconstituted DKO cells (n = 1,000 cells in random fields per experiment). The fraction of DKO+vector cells with sharp perimeters containing F-actin microspikes was 32 ± 11% at 20 min of spreading, whereas 72 ± 15% of the DKO+c-Abl cells contained microspikes at the same time point (P = 0.009, z-test). A time-course analysis performed at room temperature to slow the spreading process revealed that the DKO+vector cells formed microspikes transiently at early time points (5 min after attachment) during spreading (unpublished data). The presence of c-Abl in DKO cells extended the duration of the microspikes such that when the DKO+vector cells were flattened with smooth surface membranes, the DKO+c-Abl cells were less flattened and had numerous microspikes (Fig. 1 A shows a representative experiment). Additionally, vinculin, a cytoskeletal protein found in focal adhesions, was distributed differently in each cell type during cell spreading (Fig. 1 B). The DKO+vector cells had vinculin staining in distinct aggregates throughout the cytoplasm and cell periphery, whereas the DKO+c-Abl cells had heavy stain-

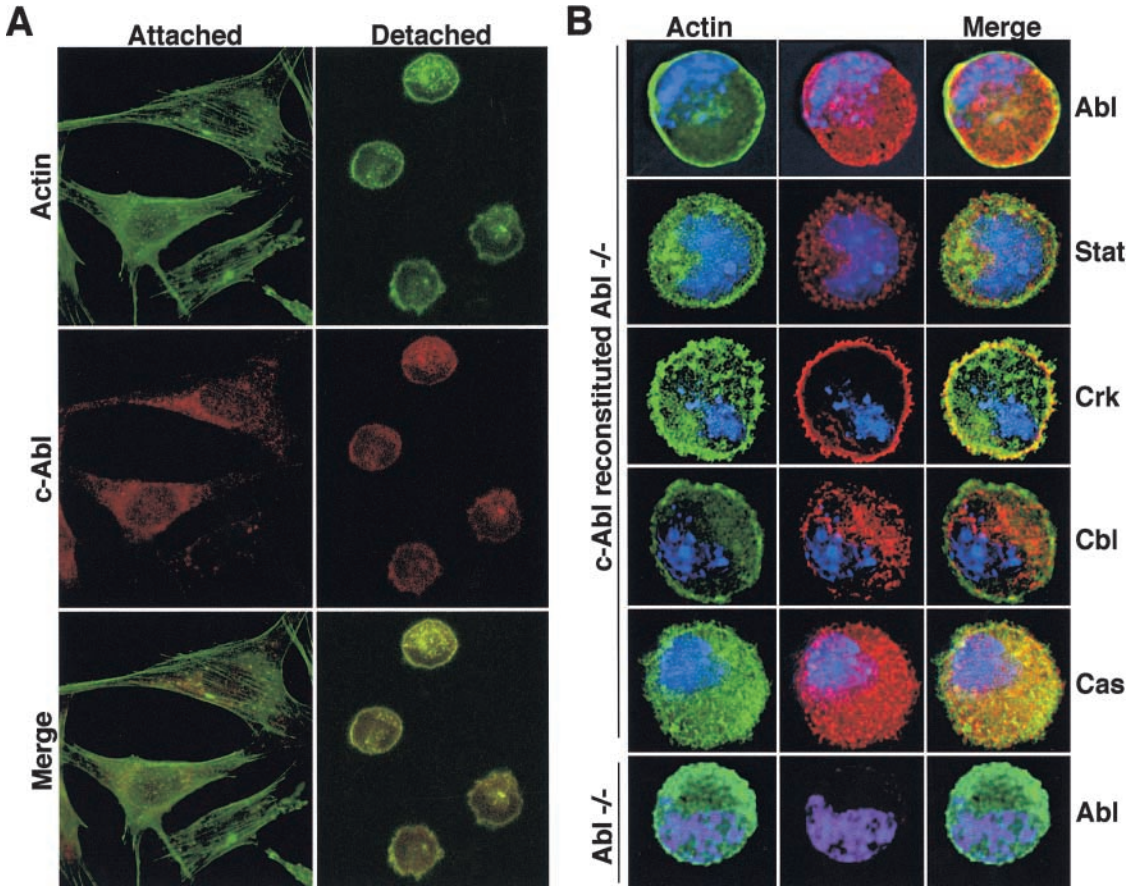

Figure 3. **Localization of c-Abl and F-actin in attached and detached c-Abl–reconstituted Abl−/− fibroblasts**. (A) Confocal images of attached (left) and detached cells (right). c-Abl–reconstituted knock out cells were detached then either replated onto fibronectin-coated coverslips or held in suspension for 45 min. Adherent cells were fixed attached to the coverslip and detached cells were fixed in suspension. Cells were stained with α8E9/αmouse Texas red and FITC-conjugated phalloidin to visualize c-Abl and F-actin respectively. Vertical plane of focus is near the top surface of cells. (B) Deconvolution images of individual detached cells. Vertical plane of focus is near the cell center for Abl staining. The antibody used for staining (in combination with Texas red secondary antibody) is indicated on the right. FITC-conjugated phalloidin and Hoechst were used to stain F-actin and the nucleus, respectively.

ing at the cell center and within the microspikes at the periphery. Furthermore, STI571, an inhibitor of c-Abl kinase, reverted the morphology of the DKO+c-Abl cells to resemble the DKO+vector cells (Fig. 1 C). Although the occurrence of the F-actin microspikes was significantly reduced by STI571 in the DKO+c-Abl cells (from 75 ± 12% to 38 ± 9%, $P = 0.003$, z-test), STI571 did not affect the morphology of the DKO+vector cells (Fig. 1 C). Thus, the effects that c-Abl has on cytoskeletal morphology of spreading fibroblasts are dependent on c-Abl kinase activity.

To address the specificity of c-Abl in microspike formation, we examined if another tyrosine kinase, c-Src, could cause similar effects during cell spreading. Mouse embryo fibroblasts deficient for c-Src were stably reconstituted with c-Src using the retroviral-mediated transfer technique described above. As observed by other investigators (e.g., Kaplan et al., 1995), reconstitution of c-Src into the Src−/− background caused cells to flatten out more rapidly on fibronectin (Fig. 1 D, top). However, microspikes were present during the spreading regardless of c-Src. Again, the presence of microspikes could be decreased by STI571 in these cells, indicating that c-Abl kinase activity contributes to formation of microspikes in c-Src−/− fibroblasts as well. We also tested the effects of an inhibitor selective for the Src family of kinases (c-Yes, Fyn, c-Src) during cell spreading (Blake et al., 2000). At 1 μM SU6656, we observed an overall decrease in the rate of cell flattening in both DKO+c-Abl and c-Src reconstituted fibroblasts, but no effect on the occurrence of F-actin microspikes (Fig. 1 D, middle). This result further suggests that Src kinases are not required for microspike formation in spreading fibroblasts. Since it has been reported that overproduction of activated Src stimulates c-Abl kinase in 293T cells (Plattner et al., 1999), we examined the formation of microspikes in this experimental system. Indeed, we found that overexpression of the activated SrcY529F mutant in 293T cells increased microspike formation, but this effect was blocked by STI571 pretreatment. Altogether, these data show that microspike formation during fibroblast spreading is specific to c-Abl kinase activity. Moreover, upon overexpression in 293T cells, activated Src could contribute to microspike formation in a manner dependent on Abl kinase activity.

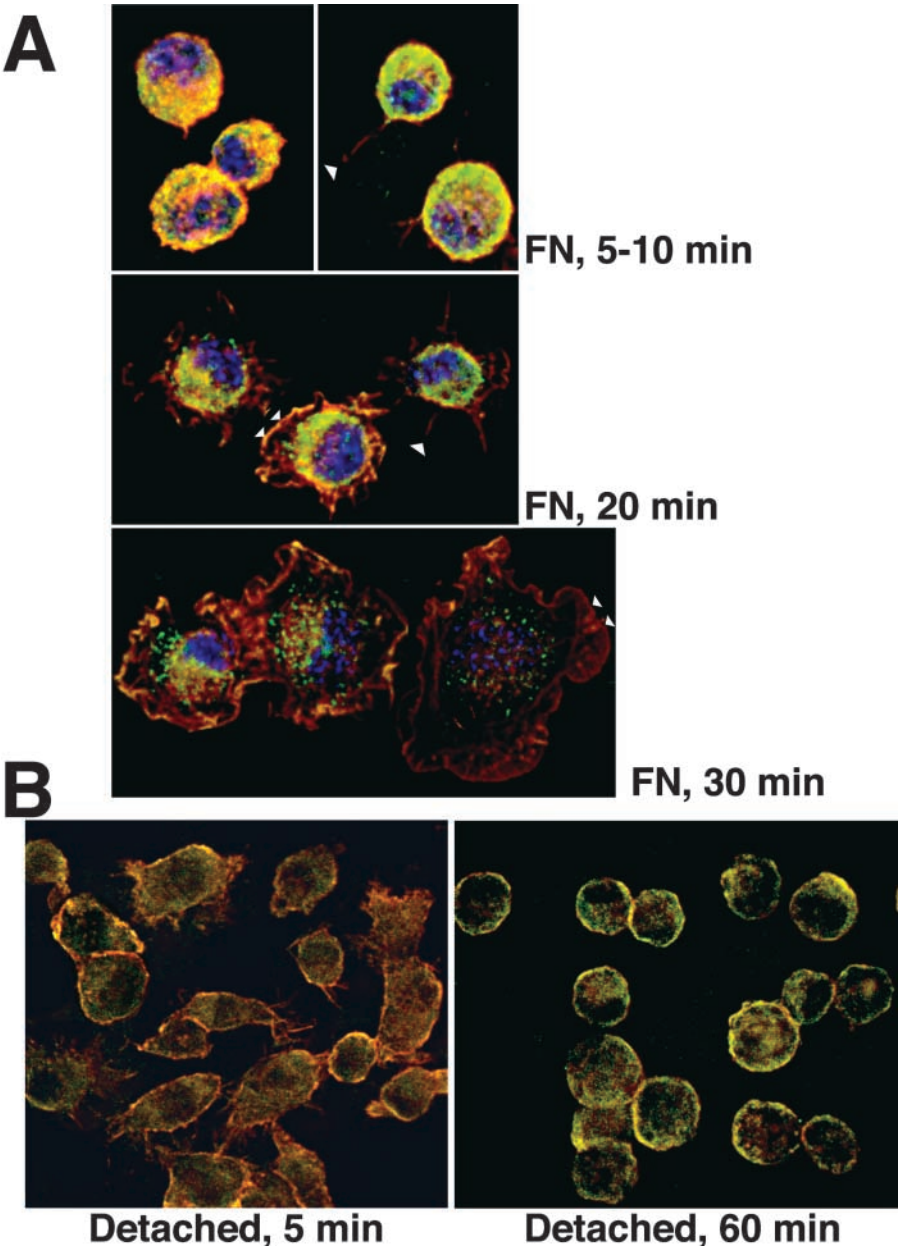

Figure 4. **Localization of c-Abl and F-actin in spreading NIH3T3 fibroblasts.** (A) NIH3T3 cells were detached, held in suspension for 40 min then reattached to a fibronectin-coated surface. Cells were fixed at the indicated times and stained with TRITC-conjugated phalloidin and α8E9/FITC-αmouse. Arrowheads indicate the F-actin–rich filopodia and lamellipodia apparent in spreading fibroblasts. (B) NIH3T3 cells were detached and held in suspension for either 5 or 60 min. Cells were fixed in suspension then stained as in A.

In vivo association of c-Abl with F-actin is affected by cell adhesion

We have shown previously that F-actin binds to and inhibits the c-Abl tyrosine kinase. Moreover, deletion of the F-actin binding domain of c-Abl increases kinase activity in detached cells (Woodring et al., 2001). These results would predict that c-Abl is associated with F-actin in detached cells. Indeed, we observed a time-dependent increase in the amount of actin found in anti-Abl immunoprecipitates as cells were held in suspension (Fig. 2 A). After 40 min in suspension, the amount of actin in the anti-Abl immunoprecipitates was 2.7 ± 0.7-fold higher than that at 5 min after detachment (Fig. 2 A, lanes 3 and 5). The increased actin in the anti-Abl precipitates corresponded with a decrease in c-Abl kinase activity (Fig. 2 B). Coimmunoprecipitation of actin and c-Abl was also observed to a limited extent in attached cells. However, a majority of this coprecipitation was also observed in anti-Abl immunoprecipitates prepared from Abl−/− cells, suggesting a nonspecific trapping of actin (Fig. 2 C, lanes 1 and 2).

The localizations of c-Abl and F-actin were examined in attached and detached cells by immunofluorescence staining (Fig. 3 A). In attached cells, the majority of the c-Abl staining appeared to be cytoplasmic, and there was little colocalization with F-actin, although there were some visible cytoplasmic aggregates that stained for both F-actin and c-Abl (Fig. 3 A, left). In contrast, in detached cells we observed a similar localization of a portion of c-Abl and F-actin at the cell perimeter (Fig. 3 A, right). Individual detached cells were also visualized in more detail at several optical planes along the vertical z-axis. We consistently observed c-Abl and F-actin staining at the cell perimeter within the same optical plane of section (a representative cell is shown in Fig. 3 B, row 1, and Figure S1, available at http://www.jcb.org/cgi/content/full/jcb.200110014/DC1).

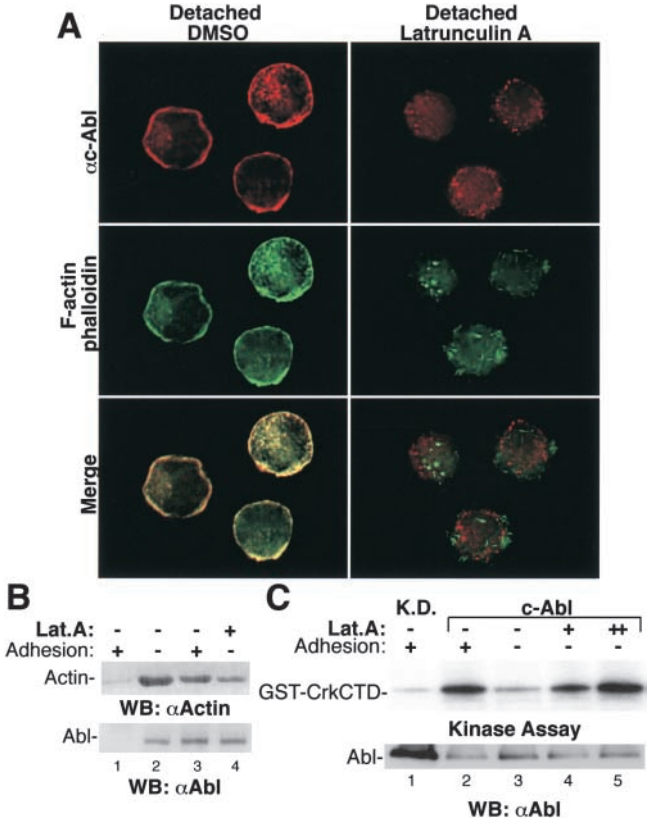

Figure 5. **Effect of Latrunculin A on c-Abl association with F-actin and c-Abl activity.** (A) Deconvolution images of detached and latrunculin A–treated detached c-Abl–reconstituted Abl−/− cells. 2 h before detachment 1 μM latrunculin A was added to media and was present throughout the suspension incubation of 40 min. Reagents used in cell staining are as indicated on the left. Vertical plane of focus is near top surface of cells. (B) c-Abl was immunoprecipitated from c-Abl reconstituted Abl−/− fibroblasts which were either detached (lane 2), fibronectin reattached (lane 3), or detached and treated with 1 μM latrunculin (lane 4) as described in A. Abl−/− cells were used as the negative control (lane 1). αactin (Sigma-Aldrich) immunoblotting and αAbl (8E9) immunoblotting of the membranes containing c-Abl immunoprecipitates are shown in the top and bottom panels, respectively. (C) c-Abl was immunoprecipitated from c-Abl reconstituted Abl−/− fibroblasts with αFLAGM2 to measure kinase activity. GST-CrkCTD was used as the Abl substrate in kinase reactions (Gong et al., 1999; Woodring et al., 2001). Latrunculin A treatment was as indicated in A, using concentrations of 0.25 μM (lane 4) or 1 μM (lane 5). DMSO was added to control cells (lanes 1–3).

We performed two controls to address specificity of c-Abl staining in detached cells. First, no detectable c-Abl staining was observed in Abl−/− cells using the 8E9 c-Abl antibody (Fig. 3 B, bottom). Second, we compared the localization of other cytosolic proteins with F-actin in detached cells (Fig. 3 B, rows 2–5). We observed localization of F-actin with Crk and to some extent with p130Cas at the cell perimeter, but not with Stat1 or c-Cbl. This indicates that some, but not all, proteins are localized to the actin cytoskeleton in detached cells. It should be noted that F-actin severing proteins such as cofilin can compete with phalloidin for binding to F-actin, and thus phalloidin staining may not reveal all of the cellular F-actin (Bamburg, 1999; McGough et al., 1997). Nonetheless, the close proximity of c-Abl and the detectable F-actin in detached cells provides evidence that c-Abl is localized to the correct position in cells to interact with and be affected by F-actin.

A time-dependent increase in c-Abl activity was observed previously when detached NIH3T3 cells were reattached and spread on fibronectin (Lewis et al., 1996). Therefore, we examined the localization of F-actin and c-Abl during the spreading process. At early times after reattachment onto fibronectin, a significant amount of association between c-Abl and F-actin remained (Fig. 4 A, top). At this early time point cells appeared contracted in a rounded morphology with smooth perimeters, although some cells had sprouted F-actin microspikes (arrows). During spreading, membranes of most cells extended into lamellipodia-like and filopodia-like structures (arrowheads, middle panel). F-actin staining was observed within the lamellipodia-like structures and throughout the cytoplasm, whereas c-Abl staining remained mostly cytoplasmic with occasional staining detectable at the ruffling edge of the membrane. At the later times of spreading, c-Abl staining was localized to cytoplasmic aggregates, whereas the F-actin staining was localized to the lamellipodia-like structures and also to cytoplasmic aggregates. Some of these aggregates contained both c-Abl and F-actin, but most contained c-Abl or F-actin. We quantified the pixels that overlapped between the F-actin and c-Abl staining using Deltavision software. Suspended cells or cells attached for 5–10 min contained 21 ± 2.8% overlap between c-Abl and F-actin, whereas cells allowed to spread for 20 min contained 12 ± 2.6% overlap and cells allowed to spread for 30 min contained 3.7 ± 2.6% overlap. The decrease in colocalization between c-Abl and F-actin correlates with the previously observed increase in Abl activity (Lewis, et al., 1996). Additionally, we examined the localization of c-Abl and F-actin in detached NIH3T3 cells held in suspension for 5 versus 60 min. Analogous to the coimmunoprecipitation result (Fig. 2), cells held in suspension for 5 min exhibited weak colocalization of c-Abl and F-actin compared with cells held in suspension for 60 min (Fig. 4 B). Together, these results suggest that in suspended cells, c-Abl colocalizes with F-actin. Following integrin activation, c-Abl begins to dissociate from F-actin and remains dissociated in attached cells at steady-state.

F-actin organization affects c-Abl activity

If F-actin is responsible for the reduction of c-Abl kinase activity, then, disruption of F-actin/c-Abl association should activate the c-Abl kinase. Therefore, we examined the effects of latrunculin A, which associates with actin monomers, preventing them from incorporating into F-actin (Morton et al., 2000) on c-Abl activity and localization. Latrunculin diminished but did not eliminate phalloidin staining, and it caused F-actin to appear as aggregates at the cell periphery (Fig. 5 A). Unlike detached cells, very little colocalization between c-Abl and F-actin was observed in latrunculin-treated cells. Loss of association of c-Abl and F-actin in latrunculin-treated cells was also confirmed by coimmunoprecipitation experiments (Fig. 5 B). Correspondingly, latrunculin treatment increased the activity of c-Abl isolated from detached cells (Fig. 5 C, compare lanes 3–5). At 1 μM

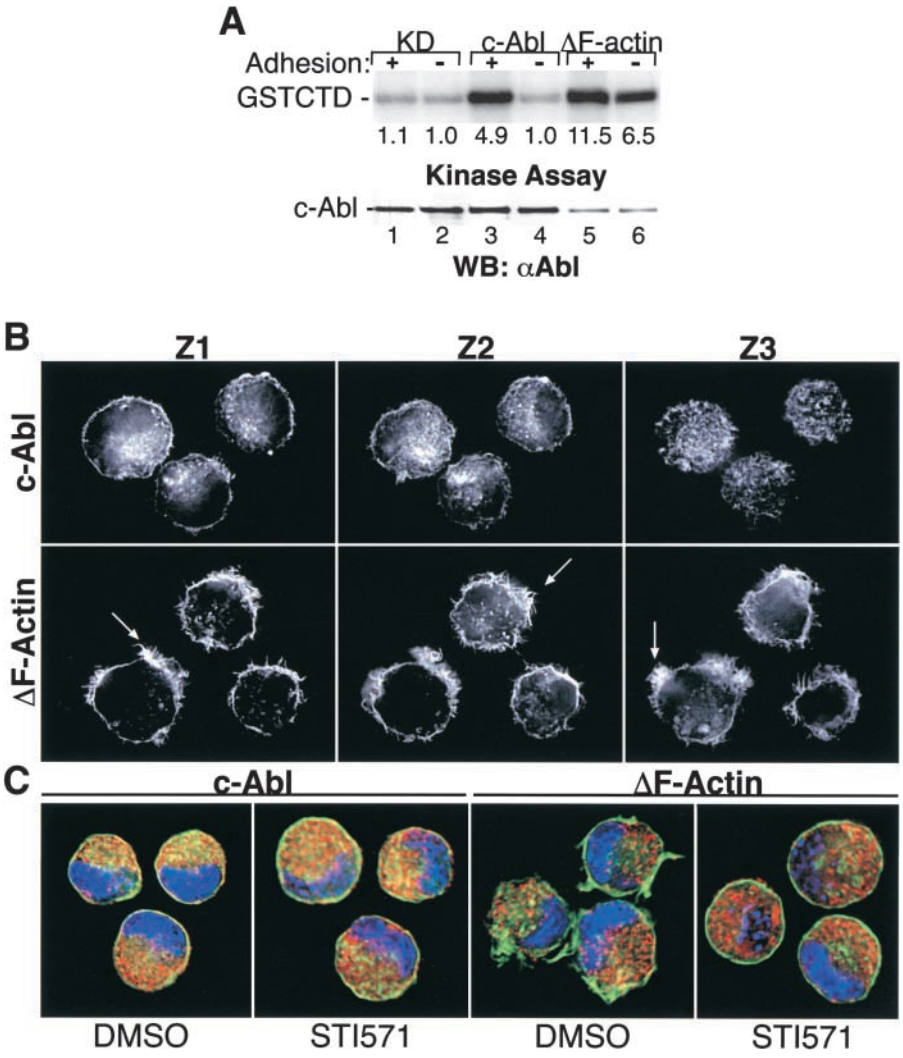

Figure 6. **Actin microspikes project from membranes of detached cells expressing ΔF-actin c-Abl.** (A) The indicated c-Abl DNA constructs were stably expressed in Abl−/− fibroblasts. Cells were detached from the substratum, then either held in suspension (Adhesion −) or attached to a fibronectin-coated surface (Adhesion +) for 40 min. c-Abl protein was immunoprecipitated (K12 antibody) and assayed for ability to phosphorylate GST-CTD of RNA polymerase II. Top panel shows the ^{32}P autoradiogram obtained after the proteins were transferred to PVDF membrane and exposed to film. Bottom panel shows the immunoblot performed on the same membrane. 8E9 antibody was used to determine the quantity of c-Abl in each immunoprecipitation. The specific activity indicated below autoradiograms is equal to (^{32}P-GST-CTD)/(c-Abl). (B) c-Abl or ΔF-actin c-Abl–reconstituted Abl−/− cells were detached, fixed in suspension, and gently centrifuged onto slides using a cryospin centrifuge. FITC-conjugated phalloidin staining was performed to visualize the F-actin cytoskeleton. Using deconvolution microscopy a Z-series of images was compiled from 0.3-μm interval images obtained along the z-axis (varying up and down the vertical focus). Z2 represents the image obtained at or near the cell center; Z1 and Z3 represent the same image 1.8 μm above and below Z2, respectively. At all optical sections examined we observed differences between the cell membranes of c-Abl versus ΔF-actin-Abl–reconstituted cells. (C) The indicated cells were pretreated with 3 μM STI571 or DMSO control for 8 h previous to cell detachment, then prepared as described in A. Fixed cells were stained with α8E9/αmouse Texas red, FITC-conjugated phalloidin, and Hoechst 33258 to visualize c-Abl, F-actin, and the nucleus, respectively.

latrunculin, the level of activity was comparable to that observed in attached cells. The effect of latrunculin is consistent with c-Abl inhibition by F-actin.

ECM-independent formation of actin microspikes in cells expressing a deregulated c-Abl kinase

Since c-Abl expression resulted in F-actin microspike formation during fibronectin-stimulated spreading (Fig. 1) and since mutation of the F-actin binding domain of c-Abl (ΔF-actin-Abl) restores c-Abl activity to detached cells (Woodring et al., 2001), we examined the cytoskeleton of detached cells expressing ΔF-actin–Abl. Detached Abl−/− cells (knock out, KO) reexpressing wild-type c-Abl (KO+c-Abl) contained basal levels of c-Abl activity, whereas detached cells expressing ΔF-actin–Abl (KO+ΔF-actin-Abl) had sixfold more activity when normalized for Abl protein (Fig. 6 A). The ΔF-actin–Abl protein was expressed at a lower level than c-Abl. This was consistently observed with this mutant protein either in infection or transfection experiments. The ΔF-actin–Abl protein is likely to be less stable, consistent with the proposed notion that activated Abl is downregulated (Echarri and Pendergast, 2001) and can contribute to apoptosis (Wang, 2000; unpublished data). Both cell types appeared rounded in suspension. However, the surface of detached cells expressing active ΔF-actin–Abl contained numerous F-actin microspikes (Fig. 6 B, arrows). Although peripheral microspikes were evident in the KO+c-Abl cells, their length and quantity were less than that observed in the KO+ΔF-actin–Abl cells. Pretreatment with STI571 caused the membranes of the KO+ΔF-actin-Abl–detached cells to resemble those of the KO+c-Abl–detached cells (Fig. 6 C) reducing both the quantity and the length of the actin microspikes. Thus, deletion of the FABD function not only allows c-Abl to remain active in detached cells, but also increases F-actin microspike protrusions on the surface of detached cells in the absence of integrin–ECM engagement.

Inhibition of Rho family GTPases does not prevent formation of Abl-dependent F-actin microspikes

GTPases such as Rac, Rho, and Cdc42 are intimately involved in regulating the F-actin cytoskeleton by promoting the formation of lamellipodia, stress fibers, and filopodia, respectively (Hall, 1998). To determine if Rho family of GTP-

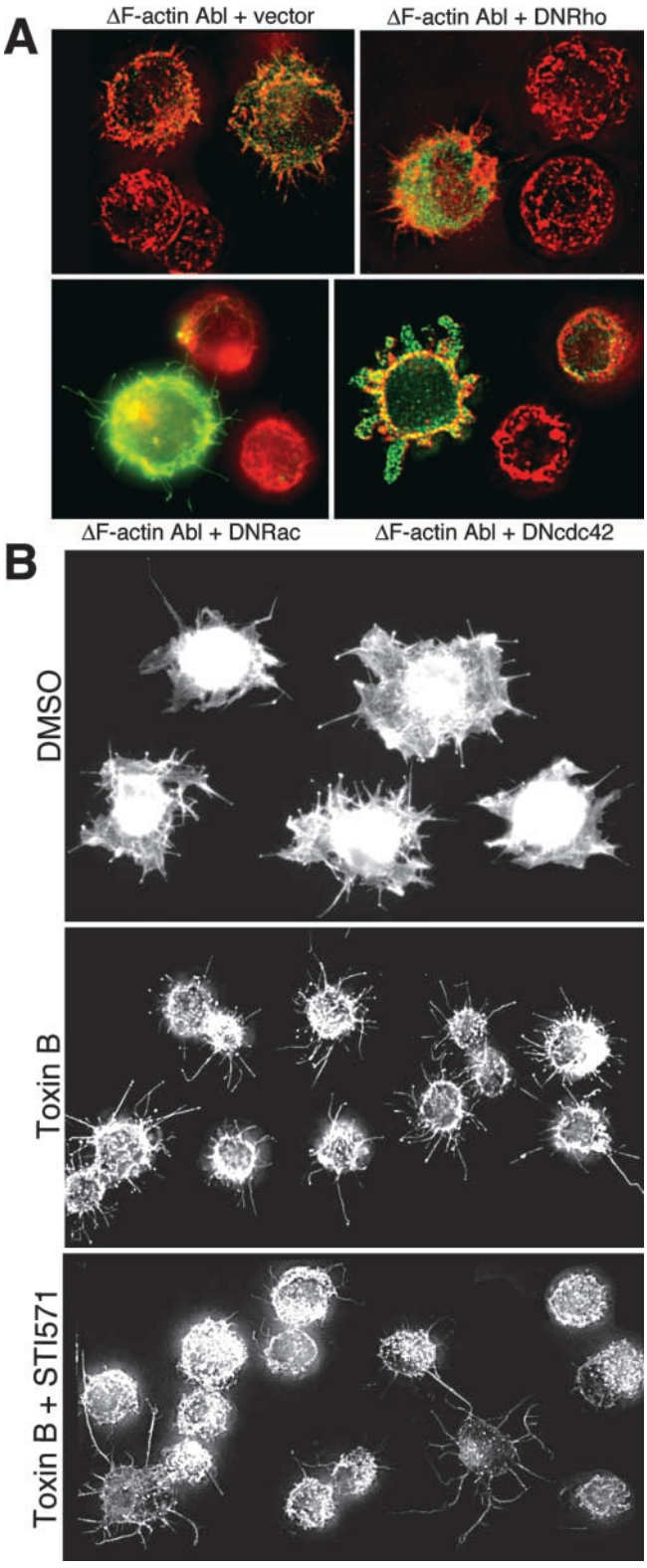

Figure 7. **Effect of dominant negative GTPases on F-actin microspikes stimulated by ΔF-actin–Abl.** (A) 293T cells were cotransfected with ΔF-actin–Abl (1 μg) and the indicated dominant negative Rho family GTPase (5 μg). Top panels are stained with α8E9/FITC-αmouse and TRITC-conjugated phalloidin, and successfully transfected cells were stained green for ΔF-actin–Abl. Bottom panels are stained with αRac/FITC-αmouse (left) and αCdc42/FITC-αrabbit, to detect successfully transfected cells, and with TRITC-conjugated phalloidin. (B) DKO+c-Abl cells were pretreated overnight with DMSO, 4 ng/ml Toxin B or 3 μM STI571 + 4 ng/ml Toxin B as indicated. Cells were detached, held in suspension for 45 min, then reattached onto fibronectin coated coverslips in the continued presence of drugs. 20 min after replating, cells were fixed and stained with TRITC-conjugated phalloidin.

ases are required in c-Abl–dependent formation of F-actin microspikes, we coexpressed ΔF-actin–Abl with dominant negative versions of each GTPase in 293T cells (Fig. 7 A). ΔF-actin–Abl expression increased the quantity of F-actin microspikes when overexpressed in transfected 293T cells. Coexpression of DNRhoA, DNRac1, or DNCdc42 with ΔF-actin–Abl did not affect the quantity of microspikes in detached cells 293T cells. However, DNRac1 and DNCdc42 influenced the morphology of the microspikes. DNRac1 appeared to lengthen microspikes, whereas DNCdc42 caused microspikes to appear broader and flatter in morphology. We also tested the effect of *Clostridium difficile* Toxin B, which inactivates Rac, Rho, and Cdc42 GTPases through ADP ribosylation on the Abl-dependent microspike formation during cell spreading (Fig. 7 B). Toxin B completely blocked the flattening of DKO+c-Abl cells onto fibronectin. However, it did not eliminate the formation of F-actin microspikes in the c-Abl–positive cells. By contrast, STI571 pretreatment of Toxin B–treated cells reduced the fraction of cells that contained F-actin microspikes. Together, these results indicate that Abl kinase activity can stimulate the formation of F-actin microspikes under conditions where the activity of Rho family GTPases was inhibited.

c-Abl affects the F-actin branching of cortical embryonic neurons

Since actin microspikes resemble the filopodia that extend from growing neurites, we examined the effects of c-Abl on the morphology of the F-actin cytoskeleton in neurons. In dissociated cultures of rat embryonic day 18 (E18) cortical neurons we found c-Abl localized to the cytoplasm throughout the neuronal cell body and extending neurites (unpublished data) similar to a previous report (Zukerberg et al., 2000). We examined the length and morphology of F-actin microspikes protruding from the longest neurite of neurons grown in the presence of DMSO or STI571 (Fig. 8 A and Table I). For simplicity we will refer to F-actin microspikes that form branch-like structures as branches. We defined a branch as an extension from a neurite that stained positive with phalloidin and was at least 2 μm in length (Fig. 8 B, arrowheads point at the base of each branch). While cortical neurons grown in primary culture for 2 d developed neurites with or without STI571, the longest neurites of STI571-treated neurons were on average 21 ± 9% shorter than those of the DMSO-treated neurons (n = 300 neurons each). This is consistent with previous observations that Abl activity can increase neurite outgrowth (Zukerberg et al., 2000). Notably, neurons treated with STI571 had a reduced number of F-actin branches extending from the longest neurites (Fig. 8, A and B). To quantify the branching we counted the number of branches along the longest neurite of DMSO- and

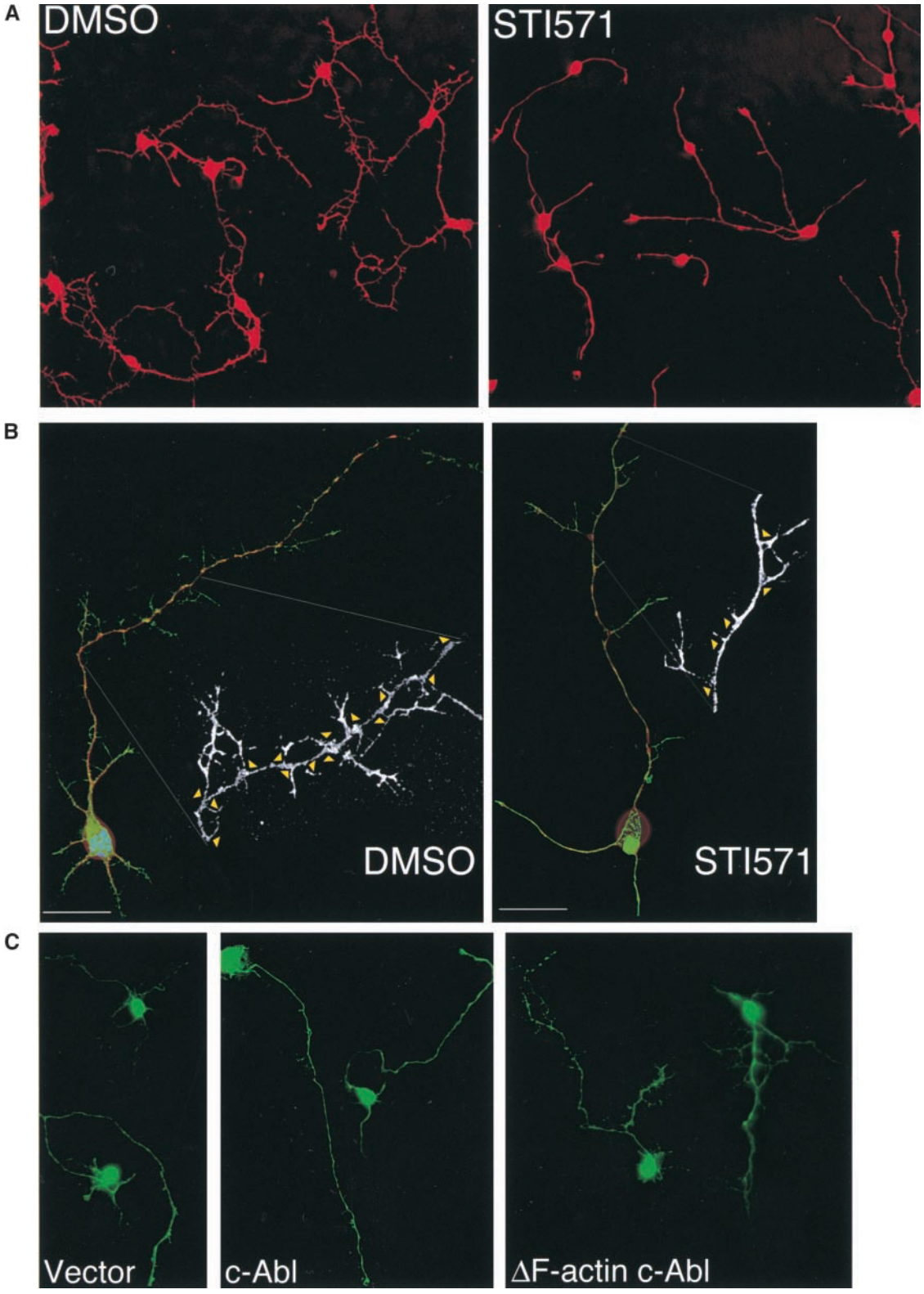

Figure 8 continues on next page

STI571-treated neurons (Fig. 8 D, top). To normalize for the shorter length of STI571-treated neurites, the data are represented as number of branches observed over a 10-μm distance. The fraction of neurons showing two or more branches over a 10-μm distance of neurite was 90% for DMSO-treated and 13% for STI571-treated. With STI571 treatment, the majority of the neurons had on average threefold fewer branches (Fig. 8 D, top).

We then transiently overexpressed c-Abl and ΔF-actin–Abl in the E18 cortical neurons, using GFP expression to

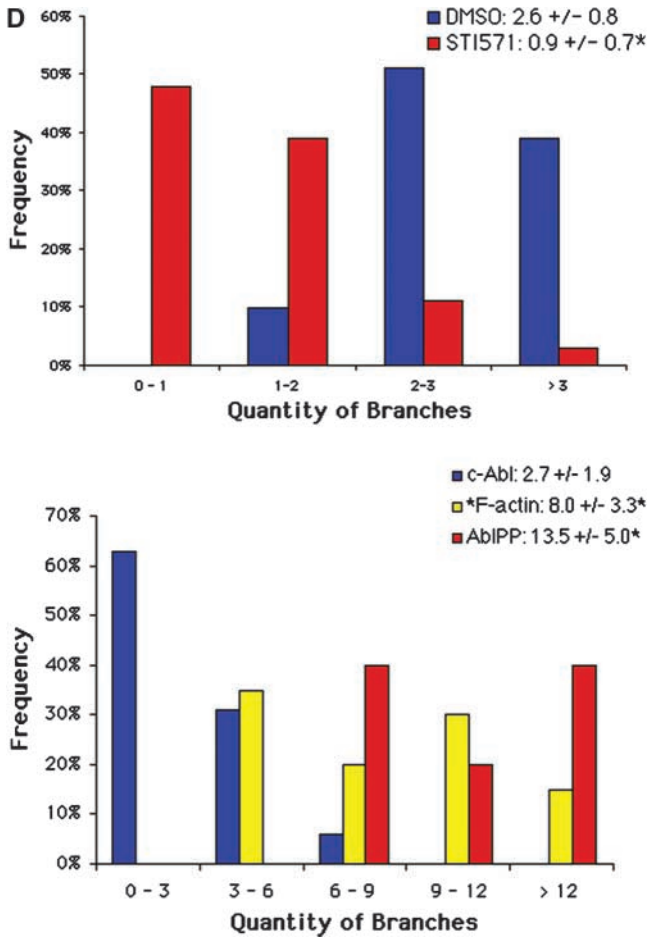

Figure 8. **Effects of STI571 and expression of ΔF-actin c-Abl on the F-actin cytoskeleton of rat embryonic cortical neurons.** (A and B) Dissociated rat E18 cortical neurons were plated onto coverslips and grown in the presence of either DMSO or 3 μM STI571 for 48 h before fixation. Fixed neurons were stained with TRITC-phalloidin (A) or αneurofilament/αrabbit-Texas red and FITC-conjugated phalloidin (B). The enlargement of a portion of the neurite in B is the phalloidin stain only. (C) Neurons were transfected 18 h after plating onto coverslips. Cotransfections were performed using Lipofectamine 2000. Left, GFP + vector; middle, GFP + c-Abl; right, GFP+ ΔF-actin c-Abl. Each panel shows two representative transfected neurons. (D) Quantification of the data provided in A and C. Neurite branches were defined as ≥2 μm F-actin protrusions present on the longest neurite of neurons. Values reported are the percentage of total neurons examined for one of three representative experiments; average reported (top right inset) is the average number of branches per 10 μm of axon length. Top, $n = 131$ neurons for DMSO; $n = 153$ neurons for STI571; asterisk indicates a $P < 0.01$, z-test. Bottom, after 12 h in culture, rat E18 cortical neurons were cotransfected with GFP DNA and the indicated c-Abl DNA. Transfected neurons were grown for an additional 48 h then stained with TRITC-phalloidin. $n = 20$ neurons for each transfection; asterisk indicates $P < 0.01$ compared with wild-type c-Abl, Student's *t* test.

identify successfully transfected cells. Relative to vector-transfected cells, the expression of wild-type c-Abl did not cause obvious phenotypic differences in neurons (Fig. 8 C). However, expression of ΔF-actin–Abl or dominant active c-Abl (c-Abl-PP, proline to glutamic acid point mutations within the SH2-catalytic domain linker) caused extensive F-actin branching relative to vector or c-Abl–transfected cells (Fig. 8 C). We observed three- and fivefold more branches on neurites expressing ΔF-actin–Abl and c-Abl–PP, respectively (Fig. 8 D, bottom).

Table I. **Branching in embryonic cortical neurons from mice deficient for Abl**

Genotype	Treatment	Neurite branches	Neurite length
abl+/*abl*+	DMSO	7.0 ± 5.3	133 ± 60
	STI571	2.2 ± 2.3[a]	112 ± 54[a]
abl+/*abl*−	DMSO	5.3 ± 3.5	129 ± 48
	STI571	1.5 ± 1.6[a]	109 ± 42[a]
abl−/*abl*−	DMSO	3.0 ± 2.8	134 ± 57
	STI571	3.3 ± 3.1	124 ± 59

$n = 200$ neurons per treatment from each of two individual E17 embryos.
[a]$P < .01$ relative to DMSO treatment for each genotype, z-test.

To further explore the role of c-Abl in neurite branching and to address the specificity of STI571 for c-Abl, we cultured dissociated cortical neurons from E17 mouse embryos which were *abl*+/+, *abl*+/− and *abl*−/− for Abl expression (see Materials and methods). We observed a twofold reduction in the number of F-actin branches on the neurites on cells from Abl−/− embryos (Table I). STI571 had no to little affect on the already low number of branches on Abl−/− mouse embryo neurons, whereas it significantly decreased branching of Abl+/− and Abl+/+ mouse embryo neurons. Consistently, as the dosage of Abl decreased, we observed significant reduction in neurite branching (Table I, compare control-treated neurons for each genotype). These data strongly imply a role for c-Abl in processes that involve dynamic changes in the F-actin cytoskeleton of neurons.

Discussion

Regulation of c-Abl kinase by F-actin

c-Abl can bind to F-actin through a consensus binding region located in the extreme COOH terminus (McWhirter and Wang, 1993; Van Etten et al., 1994; Woodring et al., 2001). Deletion of the last 4 (or 32) amino acids of c-Abl is sufficient to disrupt the binding of c-Abl to F-actin and restore c-Abl activity to suspended cells (Fig. 6). In vitro, F-actin can bind to and inhibit purified c-Abl (Woodring et al., 2001). We show here that there is an analogous correlation between F-actin association with c-Abl and decreased c-Abl activity in vivo during cell detachment. The concentration of F-actin is decreased upon cell detachment from the ECM (Clark et al., 1998). However, there is sufficient quantity of F-actin (~50 μM) in detached cells to inhibit c-Abl as the K_i for inhibition of c-Abl by F-actin is 0.5 μM (Woodring et al., 2001). Since simple mass action cannot explain the inhibition of c-Abl by F-actin in vivo, the accessibility of c-Abl for F-actin binding may be crucial. The binding of c-Abl to F-actin may be actively suppressed in attached cells despite the higher overall F-actin concentration. This could be through the sequestration of c-Abl away from F-actin or a direct inhibition of the F-actin binding activity of c-Abl. Alternatively, the inhibitory effect of F-actin on c-Abl kinase activity might be neutralized. In this regard, it is noteworthy that an activated form of Abl, Bcr-Abl kinase, is active despite its stable associ-

ation with F-actin (McWhirter and Wang, 1991, 1993), supporting the idea that the inhibitory effect of F-actin on Abl can be neutralized without dissociation.

Regulation of the F-actin cytoskeleton by c-Abl

Our data, together with those from other laboratories, imply a role for c-Abl in the dynamic organization of the F-actin cytoskeleton. With multiple approaches, we have obtained direct evidence that c-Abl kinase activity positively regulates the F-actin cytoskeleton. Using a small molecule inhibitor for c-Abl kinase, we demonstrated that inhibition of endogenous c-Abl activity not only blocked formation of F-actin microspikes in spreading fibroblasts, but also reduced F-actin branching in embryonic cortical neurons. Conversely, expression of activated c-Abl increased the quantity of microspikes in fibroblasts and increased branching of neurons. Moreover, neurons derived from mouse embryos lacking c-Abl exhibited decreased branching relative to littermate controls.

The stimulatory effect of c-Abl on branching of murine and rat embryonic cortical neurons reported in this study is consistent with the proposed positive regulatory role of dAbl in growth cone dynamics. dAbl is involved in axon outgrowth/guidance (Gertler et al., 1989; Henkemeyer et al., 1990; Gertler et al., 1995; Comer et al., 1998; Wills et al., 1999a; Bashaw et al., 2000; Bear et al., 2001) and specific motor neurons in dAbl−/− *Drosophila* undergo growth cone arrest similar to the phenotype observed in profilin−/− *Drosophila* (Wills et al., 1999b). Genetic evidence has established a connection between dAbl and molecules known to regulate F-actin dynamics of neurons. This is supported by the dosage-sensitive effects between *dAbl* and *profilin* (Wills et al., 1999b), *trio* (Rac/Rho GEF) (Liebl et al., 2000), *disabled* (*dab*) (Gertler et al., 1989), *failed axon connections* (*fax*) (Hill et al., 1995), *enabled* (*ena*) (Gertler et al., 1990, 1995; Comer et al., 1998; Wills et al., 1999a; Bashaw et al., 2000) and *Dlar* (Wills et al., 1999a). Murine c-Abl has also been implicated in the regulation axon outgrowth. Overexpression of activated c-Abl can stimulate neurite outgrowth (Zukerberg et al., 2000), whereas Abl−/−Arg−/− mouse embryos die at E11 due to defects in neurulation associated with gross actin cytoskeletal abnormalities in the neuroepithelium (Koleske et al., 1998). In addition, murine disabled (mDAB) is essential in the layering of cortical neurons (Howell et al., 1999) and the murine enabled (Mena) is essential for proper axon guidance during development (Gertler et al., 1996; Lanier et al., 1999). Further evidence that murine c-Abl is involved in processes that require regulated F-actin dynamics has been reported in fibroblasts and epithelial cells where c-Abl can affect membrane ruffling (Plattner et al., 1999) and cell motility (Frasca et al., 2001; Kain and Klemke, 2001). Here, we provide evidence linking c-Abl kinase activity directly to the formation of peripheral F-actin microspikes. F-actin microspikes may be stabilized through F-actin bundling to form filopodia, highly dynamic structures with exploratory/sensory function, which are precursors to dendritic spines (Kozma et al., 1995). Indeed, c-Abl activity correlated with increased F-actin microspikes in processes that involve exploring and sensing environmental cues: fibroblasts spreading onto fibronectin and in neurons extending neurites.

Consistent with our observation that cortical neurons grown in the presence of STI571 decreased overall neurite length by ~20%, overexpression of ΔSH3Abl caused extension of neurites on neurons transfected after 2 d in culture (Zukerberg et al., 2000). In addition to this effect, we have found that overexpression of ΔF-actin c-Abl and Abl-PP caused increased branching in our analysis in which neurons were transfected immediately following attachment. The increased branching was revealed by phalloidin staining of fixed cortical neurons. Neurofilament staining did not readily detect these short F-actin–containing branches (Fig. 8 B). In live neurons, GFP-actin has been used to detect actin-rich filopodia and dendritic spines, extremely small neuronal branch–like structures along neurites that form postsynaptic contact sites (Fischer et al., 1998; Colicos et al., 2001). The actin in filopodia and dendritic spines is highly dynamic and drives rapid and continuous changes in cytoskeletal morphology (Fischer et al., 1998; Colicos et al., 2001), which are essential for neuronal pathfinding and synaptogenesis. Furthermore, the stimulatory effect of c-Abl on branch formation in neurons is consistent with a role for c-Abl in regulating growth cone dynamics, as sites of branch formation along axon shafts exhibit many of the dynamic properties of growth cones (Sato et al., 1994; Bastmeyer and O'Leary, 1996; Szebenyi et al., 1998), including a requirement for the rapid regulation of F-actin (Kalil et al., 2000).

Since c-Abl kinase activity is essential for increased F-actin microspike formation, it is likely that a substrate of c-Abl is also essential. It is noteworthy that a number of Abl substrates or Abl-binding proteins, including Crk (Nakashima et al., 1999; Escalante et al., 2000; Kain and Klemke, 2001), p130Cas (Mayer et al., 1995; Klemke et al., 1998; O'Neill et al., 2000), paxillin (Nakamura et al., 2000; Turner, 2000), Abl interactor proteins (Abi) (Stradal et al., 2001), enabled (Wills et al., 1999a; Bashaw et al., 2000; Bear et al., 2000), LAR phosphatase (Wills et al., 1999a), Scar/WAVE (Westphal et al., 2000), p190 RhoGAP (Brouns et al., 2001), Cdk5, and cables (Zukerberg et al., 2000), have been implicated in pathways which involve rearrangement of the F-actin cytoskeleton (Lanier and Gertler, 2000). For example, like c-Abl, Mena negatively regulates fibroblast motility and potentiates outgrowth of actin-rich structures in cultured murine fibroblasts (Bear et al., 2000). Additionally, PDGF-stimulated membrane ruffling requires active c-Abl (Plattner et al., 1999) and causes c-Abl to colocalize with Scar/WAVE at the ruffling cell membrane (Westphal et al., 2000).

Interestingly and unexpectedly, the effect of c-Abl on microspike formation can occur in the presence of Toxin B and dominant negative RhoA, Rac1, or Cdc42. Although these results do not rule out the possibility that c-Abl may affect F-actin morphology through GTPase-dependent mechanisms, it is noteworthy that GTPase-independent mechanisms for modulating cytoskeleton have been reported. For example, *vaccinia* virus stimulates actin motility in a Cdc42-independent manner (Moreau et al., 2000) and actin capping or severing proteins do not require GTPases to regulate polymerized actin (Pollard et al., 2000). Also, cortactin and WASp/

Scar/WAVE proteins can stimulate the nucleating activity of Arp2/3 complex in vitro in the absence of GTPases (Yarar et al., 1999; Higgs and Pollard, 2001; Uruno et al., 2001; Weed and Parsons, 2001). Altogether, these observations suggest that c-Abl may affect multiple targets that can regulate the F-actin cytoskeleton and that the downstream targets of c-Abl may be dependent on the cell context.

Reciprocal regulation between F-actin and c-Abl tyrosine kinase

Current evidence supports a role for c-Abl in physiological responses that entail the organization and reorganization of the actin cytoskeleton. Modulation of F-actin dynamics is crucial in physiological processes such as neurulation, axonal pathfinding, branching, membrane ruffling, cell spreading, and cell migration, all of which have been shown to involve c-Abl. We have found that c-Abl can stimulate F-actin microspike formation through its kinase activity, and interestingly, F-actin can in turn inhibit the kinase activity of c-Abl. This reciprocal regulation between F-actin and c-Abl provides a dynamic mechanism for modulating the F-actin structure. Signals that override the inhibitory effect of F-actin on c-Abl can stimulate the formation of microspikes. The increase in the local concentration of F-actin might then inhibit the c-Abl kinase and thus limit the life span of these Abl-dependent F-actin protrusions. Understanding how extracellular signals modulate the reciprocal regulation between F-actin and c-Abl will provide important insights on the regulation of F-actin dynamics.

Materials and methods

Plasmids

c-Abl DNA was murine, type IV. The ΔF-actin–Abl DNA used was generated by PCR-based mutagenesis using PFU DNA polymerase (Stratagene). Deletion of amino acids 1,139–1,142 was constructed by inserting STOP codons immediately following residue 1,139. This four amino acid deletion has been shown previously to disrupt Abl binding to F-actin (Van Etten et al., 1994; Woodring et al., 2001). For expression, the various c-Abl DNA constructs (kinase-defective c-Abl), wild-type c-Abl, and ΔF-actin-c-Abl were cloned into the pMSCV-hph retroviral expression plasmid (Pear et al., 1993). Stable Abl−/− and Abl−/−Arg−/− polyclonal cell lines reconstituted with kinase-defective c-Abl, wild-type c-Abl, and ΔF-actin–c-Abl were cloned as described (Woodring et al., 2001) using retroviral-mediated gene transfer. The activated c-Abl–PP used for neuronal transfection was created by excising the sequence (amino acids 156–534) containing the P242E/P249E mutations from human c-Abl (G. Superti-Furga, Cellzone, Heidelberg, Germany) and swapping it for the analogous region in murine c-Abl. Mammalian expression vectors containing cDNAs for the DNRho family members bear the mutation T17N and were obtained from Dr. Nigel Carter (Salk Institute, San Diego, CA).

Cell culture

Stable cell lines. The stable Abl-deficient fibroblast cell line Abl−/− was obtained from Dr. Rubio Ren (Brandeis University, Waltham, MA) and the stable Abl−/−Arg−/− (double knock out, DKO) cell line from Dr. Anthony Koleske (Yale University, New Haven, CT). The stable Src-deficient cell line Src−/− and Src reexpressing cells were obtained from Dr. Martin A. Broome (SUGEN, San Francisco, CA). Cells were maintained in high glucose DME supplemented with 10% fetal bovine serum, L-glutamine, and antibiotics. The DKO cell lines were plated 20 h before experiments in complete media without antibiotics. For detachment, growing cells were trypsinized at ∼75% confluency and held in suspension in DME supplemented with 1 mg/ml BSA and 0.5 mg/ml soybean trypsin inhibitor. For reattachment, suspension cells were replated onto 10 μg/ml fibronectin. For Latrunculin A (Molecular Probes) pretreatment, growth media was replaced with serum-free media containing 1 μM latrunculin for a 2 h before cell detachment. Control cells were incubated under the same conditions except with DMSO (the vehicle for the STI571). After detachment, cells were held in suspension in the same media for an additional 40 min. STI571 was added to a final concentration of 5 μM for fibroblasts or 1–3 μM for cortical neuronal cells. For fibroblasts, an 8-h pretreatment was used, and for cortical cells, STI571 was continually present in growth media from time of cell plating. Control cells were incubated with DMSO. For Toxin B pretreatment, growth media was replaced with serum-free media containing either vehicle or 4 ng/ml Toxin B (Calbiochem) for 8 h. Cells were detached and replated as described above except in the continuous presence of Toxin B.

Cortical neuronal cell culture. The cerebral cortices from E18 rats or E17 mice were dissected in L-15. Tissue was dissociated by treatment for 20 min at 27°C with 1% papain (Worthington) in HBSS (GIBCO BRL) containing 0.45% glucose, 0.2 mg/ml BSA, 0.2 mg/ml L-cysteine, 0.005% DNase I, 0.01 mg/ml APV, and 0.2 mg/ml kynurenic acid. Tissue was then washed three times in HBSS containing 0.1 mg/ml trypsin inhibitor, 0.45% glucose, 0.2 mg/ml BSA, 0.01 mg/ml APV, and 0.2 mg/ml kynurenic acid. Tissue was rinsed one time in growth medium (Neurobasal, 4% B-27, 0.5 mM glutamine, 50 U-μg/ml penicillin-streptomycin) containing 0.2 mg/ml BSA, 0.01 mg/ml APV, and 0.2 mg/ml kynurenic acid, and then triturated 20 times in 1 ml of the same medium using a fire-polished glass pipet. Dissociated cells were counted using trypan blue. Cells were plated on laminin-coated coverslips in growth medium at a density of ∼40,000 cells/cm^2 for transfections, and 4,000 cells/cm^2 for all other experiments. Transient transfections of neurons were performed with Lipofectamine 2000 reagent (GIBCO BRL) according to the manufacturer's protocol.

Biochemistry

Fibroblast experiments involving cell detachment, fibronectin stimulation, immunoprecipitation, and kinase assay were performed as described previously (Woodring et al., 2001). Antibodies used for immunoprecipitation and immunoblotting are indicated in figure legends.

Immunofluorescence staining and cell spreading

Tissue culture dishes containing glass coverslips were coated with 10 μg/ml purified fibronectin or 1 mg/ml poly-L-lysine as described previously (Schlaepfer et al., 1997). Confluent cells were detached by trypsinization and held in suspension for 40 min to inactivate c-Abl. For adherent cells, cells were plated onto washed fibronectin-coated coverslips and incubated at 37°C for the indicated times. To stop cell spreading immediately or to fix detached cells and neurons formaldehyde was added directly to the media to a final concentration of 3.7%. Fixed cells were washed gently with PBS/3.7% formaldehyde and then prepared for immunofluorescence staining as described previously (Lewis et al., 1996). Detached cells were applied to a charged surface either by allowing cells to settle to the surface or by gentle centrifugation using cryospin. FITC- or TRITC-conjugated phalloidin was used to detect F-actin; anti-8E9 and Texas red– or Cy-2–conjugated goat anti–mouse were used to detect c-Abl; and Hoechst 33258 was used to detect nuclei. Microscopy was performed using the 60× objective on an Olympus microscope unless indicated otherwise. DeltaVision (Applied Precision software) was used to deconvolve z-series images and also to measure neurite length and assess neuronal branching. For cell-spreading analysis we scored cells as either spreading with rounded or sharp cell perimeters. Antivinculin antibodies were from Sigma-Aldrich, and anti-Src monoclonal antibodies (clone 327.5) were a gift from Suzanne Simon (Salk Institute).

Online supplemental material

A supplemental figure is available at http://www.jcb.org/cgi/content/full/jcb.200110014/DC1. To examine the localization of c-Abl with the F-actin cytoskeleton in detached cells at various optical planes along the vertical z-axis, cells were stained as described in Fig. 3 B. Top, individual cells visualized with deconvolution microscopy. Bottom, field of cells visualized with confocal microscopy.

We thank Novartis for the STI571 (Gleevec™); Drs. Robert Blake and Sugen for the SU6656; Irina C. Hunton for providing the *abl*+/+, *abl*+/− and *abl*−/− mouse embryos; Dr. Giulio Superti-Furga for the c-Abl-PP construct, Suzanne Simon for the SrcY529F construct and the Src (327.5) antibodies; Dr. Anthony Koleske for the Abl−/−Arg−/− cells; Dr. Rubio Ren for the Abl−/− cells; Dr. Martin Broome for the Src−/− and reconstituted Src−/− cells; and Dr. Nigel Carter for the cDNAs encoding dominant negative versions of Rac1, RhoA, and Cdc42 and also for insightful input and scientific discussions.

This work was supported by a postdoctoral fellowship from the National Cancer Institute (NIH CA76710 to P.J. Woodring) and National Institutes of Health grants HL57900 (to J.Y.J. Wang), CA82863 (to T. Hunter), and NS31558 (to D. O'Leary). J.Y.J. Wang is the Herbert Stern Endowed Chair of Biology, University of California at San Diego. T. Hunter is a Frank and Else Schilling American Cancer Society Research Professor.

Submitted: October 2, 2001
Revised: January 22, 2002
Accepted: January 22, 2002

References

Bamburg, J. 1999. Proteins of the ADF/cofilin family: essential regulators of actin dynamics. *Annu. Rev. Cell Dev. Biol.* 15:185–230.

Bashaw, G., T. Kidd, D. Murray, T. Pawson, and C. Goodman. 2000. Repulsive axon guidance: Abelson and Enabled play opposing roles downstream of the roundabout receptor. *Cell.* 101:703–715.

Baskaran, R., G.G. Chiang, and J.Y.J. Wang. 1996. Identification of a binding site in c-Abl tyrosine kinase for the C-terminal repeated domain of RNA polymerase II. *Mol. Cell. Biol.* 16:3361–3369.

Baskaran, R., M. Dahmus, and J.Y.J. Wang. 1993. Tyrosine phosphorylation of mammalian RNA polymerase II carboxyl-terminal domain. *Proc. Natl. Acad. Sci. USA.* 90:11167–11171.

Bastmeyer, M., and D.D. O'Leary. 1996. Dynamics of target recognition by interstitial axon branching along developing cortical axons. *J. Neurosci.* 16:1450–1459.

Bear, J., M. Krause, and F. Gertler. 2001. Regulating cellular actin assembly. *Curr. Opin. Cell Biol.* 13:158–166.

Bear, J., J. Loureiro, I. Libova, R. Fassler, J. Wehland, and F. Gertler. 2000. Negative regulation of fibroblast motility by Ena/VASP proteins. *Cell.* 101:717–728.

Blake, R.A., M.A. Broome, X. Liu, J. Wu, M. Gishizky, L. Sun, and S.A. Courtneidge. 2000. SU6656, a selective Src family kinase inhibitor, used to probe growth factor signaling. *Mol. Cell. Biol.* 20:9018–9027.

Brouns, M., S. Matheson, and J. Settleman. 2001. p190 RhoGAP is the principal Src substrate in brain and regulates axon outgrowth, guidance and fasciculation. *Nat. Cell Biol.* 3:361–367.

Clark, E., W. King, J. Brugge, M. Symons, and R. Hynes. 1998. Integrin-mediated signals regulated by members of the Rho family of GTPases. *J. Cell Biol.* 142:573–586.

Colicos, M.A., B.E. Collins, M.J. Sailor, and Y. Goda. 2001. Remodeling of synaptic actin induced by photoconductive stimulation. *Cell.* 107:605–616.

Comer, A., S. Ahern-Djamali, J. Juang, P. Jackson, and F. Hoffmann. 1998. Phosphorylation of Enabled by the *Drosophila* Abelson tyrosine kinase regulates the in vivo function and protein-protein interactions of Enabled. *Mol. Cell. Biol.* 18:152–160.

Echarri, A., and A.M. Pendergast. 2001. Activated c-Abl is degraded by the ubiquitin-dependent proteosome pathway. *Curr. Biol.* 11:1759–1765.

Escalante, M., J. Courtney, W. Chin, K. Teng, J. Kim, J. Fajardo, B. Mayer, B. Hempstead, and R. Birge. 2000. Phosphorylation of c-Crk II on the negative regulatory Tyr222 mediates nerve growth factor-induced cell spreading and morphogenesis. *J. Biol. Chem.* 275:24787–24797.

Frasca, F., P. Vigneri, V. Vella, R. Vigneri, and J.Y.J. Wang. 2001. Tyrosine kinase inhibitor STI571 enhances thyroid cancer cell motile response to Hepatocyte Growth Factor. *Oncogene.* 20:3845–3856.

Fischer, M., S. Kaech, D. Knutti, and A. Matus. 1998. Rapid actin-based plasticity in dendritic spines. *Neuron.* 20:847–854.

Gertler, F., A. Comer, J. Juang, S. Ahern, M. Clark, E. Liebl, and F. Hoffmann. 1995. Enabled, a dosage-sensitive suppressor of mutations in the *Drosophila* Abl tyrosine kinase, encodes an Abl substrate with SH3 domain-binding properties. *Genes Dev.* 9:521–533.

Gertler, F., J. Doctor, and F. Hoffmann. 1990. Genetic suppression of mutations in the *Drosophila* abl proto-oncogene homolog. *Science.* 248:857–860.

Gertler, F., K. Niebuhr, M. Reinhard, J. Wehland, and P. Soriano. 1996. Mena, a relative of VASP and *Drosophila* Enabled, is implicated in the control of microfilament dynamics. 1996. *Cell.* 87:227–239.

Gertler, F.B., R.L. Bennett, M.J. Clark, and F.M. Hoffmann. 1989. *Drosophila* Abl tyrosine kinase in embryonic CNS axons: a role in axonogenesis is revealed through dosage-sensitive interactions with disabled. *Cell.* 58:103–113.

Gong, J.G., A. Costanzo, H.Q. Yang, G. Melino, W.G.J. Kaelin, M. Levrero, and J.Y.J. Wang. 1999. The tyrosine kinase c-Abl regulates p73 in apoptotic response to cisplatin-induced DNA damage. *Nature.* 399:806–809.

Hall, A. 1998. Rho GTPases and the actin cytoskeleton. *Science.* 279:509–514.

Henkemeyer, M., S.R. West, F.B. Gertler, and F.M. Hoffmann. 1990. A novel tyrosine kinase-independent function of *Drosophila abl* correlates with proper subcellular localization. *Cell.* 63:949–960.

Higgs, H.N., and T.D. Pollard. 2001. Regulation of actin filament network formation through Arp2/3 complex: activation by a diverse array of proteins. *Annu. Rev. Biochem.* 70:649–676.

Hill, K., V. Bedian, J. Juang, and F. Hoffmann. 1995. Genetic interactions between the *Drosophila* Abelson (Abl) tyrosine kinase and failed axon connections (fax), a novel protein in axon bundles. *Genetics.* 141:595–606.

Howell, B.W., T.M. Herrick, and J.A. Cooper. 1999. Reelin-induced tryosine phosphorylation of disabled 1 during neuronal positioning. *Genes Dev.* 13:643–648.

Hynes, R.O. 1992. Integrins: versatility, modulation and signaling in cell adhesion. *Cell.* 69:11–25.

Kain, K., and R. Klemke. 2001. Inhibition of cell migration by Abl family tyrosine kinases through uncoupling of Crk-CAS complexes. *J. Biol. Chem.* 276:16185–16192.

Kalil, K., G. Szebenyi, and E. Dent. 2000. Common mechanisms underlying growth cone guidance and axon branching. *J. Neurobiol.* 44:145–158.

Kaplan, K.B., J.R. Swedlow, D.O. Morgan, and H.E. Varmus. 1995. c-Src enhances the spreading of src−/− fibroblasts on fibronectin by a kinase-independent mechanism. *Genes Dev.* 9:1505–1517.

Klemke, R.L., J. Leng, R. Molander, P.C. Brooks, K. Vuori, and D.A. Cheresh. 1998. CAS/Crk coupling serves as a "molecular switch" for induction of cell migration. *J. Cell Biol.* 140:961–972.

Koleske, A.J., A.M. Gifford, M. Scott, M. Nee, R.T. Bronson, K. Miczek, and D. Baltimore. 1998. Essential roles for the Abl and Arg tyrosine kinases in neurulation. *Neuron.* 21:1259–1272.

Kozma, R., S. Ahmed, A. Best, and L. Lim. 1995. The Ras-related protein Cdc42Hs and bradykinin promote formation of peripheral actin microspikes and filopodia in Swiss 3T3 fibroblasts. *Mol. Cell. Biol.* 15:1942–1952.

Lanier, L., M. Gates, W. Witke, A. Menzies, A. Wehman, J. Macklis, D. Kwiatkowski, P. Soriano, and F. Gertler. 1999. Mena is required for neurulation and commissure formation. *Neuron.* 22:313–325.

Lanier, L., and F. Gertler. 2000. From Abl to actin: Abl tyrosine kinase and associated proteins in growth cone motility. *Curr. Opin. Neurobiol.* 10:80–87.

Lewis, J., R. Baskaran, S. Taagepera, M. Schwartz, and J.Y.J. Wang. 1996. Integrin regulation of c-Abl tyrosine kinase activity and cytoplasmic-nuclear transport. *Proc. Natl. Acad. Sci. USA.* 93:15174–15179.

Lewis, J.M., and M.A. Schwartz. 1998. Integrins regulate the association and phosphorylation of paxillin by c-Abl. *J. Biol. Chem.* 273:14225–14230.

Liebl, E., D. Forsthoefel, L. Franco, S. Sample, J. Hess, J. Cowger, M. Chandler, A. Shupert, and M. Seeger. 2000. Dosage-sensitive, reciprocal genetic interactions between the Abl tyrosine kinase and the putative GEF trio reveal trio's role in axon pathfinding. *Neuron.* 26:107–118.

Mayer, B.J., H. Hirai, and R. Sakai. 1995. Evidence that SH2 domains promote processive phosphorylation by protein-tyrosine kinases. *Curr. Biol.* 5:296–305.

McGough, A., B. Pope, W. Chiu, and A. Weeds. 1997. Cofilin changes the twist of F-actin: implications for actin filament dynamics and cellular function. *J. Cell Biol.* 138:771–781.

McWhirter, J.R., and J.Y.J. Wang. 1991. Activation of tyrosine kinase and microfilament-binding functions of c-Abl by Bcr sequences in Bcr/Abl fusion proteins. *Mol. Cell. Biol.* 11:1553–1565.

McWhirter, J.R., and J.Y.J. Wang. 1993. An actin-binding function contributes to transformation by the Bcr-Abl oncoprotein of Philadelphia chromosome-positive human leukemias. *EMBO J.* 12:1533–1546.

Moreau, V., F. Frischknecht, I. Reckmann, R. Vincentelli, G. Rabut, D. Stewart, and M. Way. 2000. A complex of N-WASP and WIP integrates signaling cascades that lead to actin polymerization. *Nat. Cell Biol.* 7:441–448.

Morton, W., K. Ayscough, and P. McLaughlin. 2000. Latrunculin alters the actin-monomer subunit interface to prevent polymerization. *Nat. Cell Biol.* 2:376–378.

Nakamura, K., H. Yano, H. Uchida, S. Hashimoto, E. Schaefer, and H. Sabe. 2000. Tyrosine phosphorylation of paxillin alpha is involved in temporospatial regulation of paxillin-containing focal adhesion formation and F-actin organization in motile cells. *J. Biol. Chem.* 275:27155–27164.

Nakashima, N., D. Rose, S. Xiao, K. Egawa, S. Martin, T. Haruta, A. Saltiel, and J. Olefsky. 1999. The functional role of CrkII in actin cytoskeleton organiza-

tion and mitogenesis. *J. Biol. Chem.* 274:3001–3008.

O'Neill, G., S. Fashena, and E. Golemis. 2000. Integrin signaling: a new Cas(t) of characters enters the stage. *Trends Cell Biol.* 10:111–119.

Pear, W.S., G.P. Nolan, M.L. Scott, and D. Baltimore. 1993. Production of high-titer helper-free retroviruses by transient transfection. *Proc. Natl. Acad. Sci. USA.* 90:8392–8396.

Plattner, R., L. Kadlec, K.A. DeMali, A. Kazlauskas, and A.M. Pendergast. 1999. c-Abl is activated by growth factors and Src family kinases and has a role in the cellular response to PDGF. *Genes Dev.* 13:2400–2411.

Pollard, T., L. Blanchoin, and R. Mullins. 2000. Molecular mechanisms controlling actin filament dynamics in nonmuscle cells. *Annu. Rev. Biophys. Biomol. Struct.* 29:545–576.

Sato, M., L. Lopez-Mascaraque, C.D. Heffner, and D.D. O'Leary. 1994. Action of a diffusible target-derived chemoattractant on cortical axon branch induction and directed growth. *Neuron.* 13:791–803.

Schlaepfer, D.D., M.A. Broome, and T. Hunter. 1997. Fibronectin-stimulated signaling from a focal adhesion kinase-c-Src complex: involvement of the Grb2, p130cas, and Nck adaptor proteins. *Mol. Cell. Biol.* 17:1702–1713.

Sotiropoulos, A., D. Gineitis, J. Copeland, and R. Tresiman. 1999. Signal-regulated activation of serum response factor is mediated by changes in actin dynamics. *Cell.* 98:159–169.

Stradal, T., K. Courtney, K. Rottner, P. Hahne, J. Small, and A. Pendergast. 2001. The Abl interactor proteins localize to sites of actin polymerization at the tips of lamellipodia and filopodia. *Curr. Biol.* 11:891–895.

Szebenyi, G., J.L. Callaway, E.W. Dent, and K. Kalil. 1998. Interstitial branches develop from active regions of the axon demarcated by the primary growth cone during pausing behaviors. *J. Neurosci.* 18:7930–7940.

Turner, C. 2000. Paxillin interactions. *J. Cell Sci.* 113:4139–4140.

Uruno, T., J. Liu, P. Zhang, Y. Fan, C. Egile, R. Li, S.C. Mueller, and S. Zhan. 2001. Activation of Arp2/3 complex-mediated actin polymerization by cortactin. *Nat. Cell Biol.* 3:259–266.

Van Etten, R.A. 1999. Cycling, stressed-out and nervous: cellular functions of c-Abl. *Trends Cell Biol.* 9:179–186.

Van Etten, R.A., P.K. Jackson, D. Baltimore, M.C. Sanders, P.T. Matsudaira, and P.A. Janmey. 1994. The COOH terminus of the c-Abl tyrosine kinase contains distinct F- and G-actin binding domains with bundling activity. *J. Cell Biol.* 124:325–340.

Wang, J.Y.J. 2000. Regulation of cell death by the Abl tyrosine kinase. *Oncogene.* 19:5643–5650.

Weed, S.A., and J.T. Parsons. 2001. Cortactin: coupling membrane dynamics to cortical actin networks. *Oncogene.* 20:6418–6434.

Westphal, R., S. Soderling, N. Alto, L. Langeberg, and J. Scott. 2000. Scar/WAVE-1, a Wiskott-Aldrich syndrome protein, assembles an actin-associated multi-kinase scaffold. *EMBO J.* 19:4589–4600.

Wills, Z., J. Bateman, C.A. Korey, A. Comer, and D. Van Vactor. 1999a. The tyrosine kinase Abl and its substrate enabled collaborate with the receptor phosphatase Dlar to control motor axon guidance. *Neuron.* 22:301–312.

Wills, Z., L. Marr, K. Zinn, C.S. Goodman, and D. Van Vactor. 1999b. Profilin and the Abl tyrosine kinase are required for motor axon outgrowth in the *Drosophila* embryo. *Neuron.* 22:291–299.

Woodring, P.J., T. Hunter, and J.Y.J. Wang. 2001. Inhibition of c-Abl tyrosine kinase by filamentous-actin. *J. Biol. Chem.* 276:27104–27110.

Yarar, D., W. To, A. Abo, and M.D. Welch. 1999. The Wiskott-Aldrich syndrome protein directs actin-based motility by stimulating actin nucleation with the Arp2/3 complex. *Curr. Biol.* 9:555–558.

Zigmond, S. 1996. Signal transduction and actin filament organization. *Curr. Opin. Cell Biol.* 8:66–73.

Zukerberg, L., G. Patrick, M. Nikolic, S. Humbert, C. Wu, L. Lanier, F. Gertler, M. Vidal, R. Van Etten, and L. Tsai. 2000. Cables links Cdk5 and c-Abl and facilitates Cdk tyrosine phosphorylation, kinase upregulation, and neurite outgrowth. *Neuron.* 26:633–646.